HHS Public Access

Author manuscript

J Am Chem Soc. Author manuscript; available in PMC 2019 April 24.

Published in final edited form as:

J Am Chem Soc. 2018 October 24; 140(42): 13534–13537. doi:10.1021/jacs.8b04843.

One-Pot Hydrothermal Synthesis of Benzalkonium-Templated Mesostructured Silica Antibacterial Agents

Viktor Dubovoy[†], **Anjani Ganti**[‡], **Tao Zhang**[‡], **Hassan Al-Tameemi**[#,§], **Juan D. Cerezo**[#], **Jeffrey M. Boyd**[#,*], and **Tewodros Asefa**[†,‡,*]

[†]Department of Chemistry and Chemical Biology, Rutgers, The State University of New Jersey, Piscataway, New Jersey 08854, United States

[‡]Department of Chemical and Biochemical Engineering, Rutgers, The State University of New Jersey, Piscataway, New Jersey 08854, United States

[#]Department of Biochemistry and Microbiology, Rutgers, The State University of New Jersey, New Brunswick, New Jersey 08901, United States

Abstract

Novel mesostructured silica microparticles are synthesized, characterized and investigated as a drug delivery system (DDS) for antimicrobial applications. The materials exhibit relatively high density (0.56 g per 1 g SiO_2) of BAC, pore channels of 18 Å in width, and high surface area (1500 m^2/g). Comparison of SAXRD pattern with BJH pore size distribution data suggests that the 18 Å pores exhibit short range ordering and a wall thickness of *ca*. 12 Å. Drug release studies demonstrate pH-responsive controlled release of BAC without additional surface modification of the materials. Prolonged drug release data was analyzed using a power law (Korsmeyer-Peppas) model and indicates substantial differences in release mechanism in acidic (pH 4.0, 5.0, 6.5) versus neutral (pH 7.4) solutions. Microbiological assays demonstrate a significant time-dependent reduction in *Staphylococcus aureus* and *Salmonella enterica* viability above 10 and 130 mg L^{-1} of the synthesized materials, respectively. The viability of cells is reduced over time compared to control samples. The findings will help in widening the use of BAC as a disinfectant and bactericidal agent, especially in pharmaceutical and food industries where Gram-positive and Gram-negative bacterial contamination is common.

Over the past several decades, mesoporous silica nanoparticles (MSNs) have attracted a great deal of interest in fields such as catalysis, drug delivery systems (DDS), sensing, environmental remediation, and nanoelectronics due to their unique structures and properties.[1–8] Since the first report of drug delivery systems based on MSNs, research on biomedical applications of MSNs has increased exponentially each year.[2,9] MSNs demonstrated significant advantages over traditional nano-based formulations for potential treatment of diabetes, inflammation, and especially cancer.[10–14] However, significant effort is still warranted to overcome the key challenges involved with developing effective DDSs

* tasefa@rci.rutgers.edu, jeffboyd@sebs.rutgers.edu.

§Current Address: College of Veterinary Medicine, University of Basrah, Basrah, Iraq

that can attain: 1) sufficient drug loading capacity, 2) controlled or activated release, 3) targeted delivery of drug, and 4) biocompatibility.

MSNs are typically synthesized with “inert” structure directing agents (SDAs), commonly referred to as soft templates, with their subsequent removal to yield nanoporous structures suitable for surface modification and drug loading. On the other hand, several previous reports have described the use of different active molecules (*e.g.*, a corrosion inhibitor, an antitumor drug, etc.) as templates for the synthesis of various porous silica materials.[15–17] Although numerous advantages of one-step fabrication of DDSs have been realized through these works, there have been only a few reports involving those with antimicrobial applications, and the efficacy of the fabricated materials is often not evaluated beyond the scope of drug release kinetics.

The bactericidal drug benzalkonium chloride (BAC) (Figure 1) forms micelles in aqueous solution above a critical micelle concentration of *ca.* 0.5 mM.[18] BAC is a ubiquitous ingredient in food, pharmaceutical, and industrial formulations due to its broad spectrum of bactericidal activity. In small concentrations, it affects the membrane permeability to cause cytolytic leakage of cytoplasmic materials (Figure 1); however, at high concentrations, it targets carboxylic groups to cause coagulation in the bacterial cytoplasm.[19] Herein, we report the development of novel BAC-templated mesoporous silica microparticles, dubbed BAC-SiO_2, for antimicrobial drug delivery by using BAC as the template during a one-step hydrothermal synthesis. The material demonstrates a relatively high payload of BAC, a sustained and prolonged release of BAC in physiologically-relevant pH ranges (4-8), an extremely high surface area framework upon removal of BAC, and a time-dependent bactericidal activity.

Synchrotron-based small-angle X-ray scattering (SAXS) and static light scattering (SLS) measurements of aqueous BAC/NH4OH solution prior to TEOS addition revealed the presence of nano-sized BAC micelle aggregates. SAXS profile (Figure S1 in Supporting Information, SI) exhibits diffraction peaks within the range of *ca.* 20-70 Å. SLS measurements (Figure S2), in decent agreement of SAXS, revealed size distribution between *ca.* 10-50 Å. The FTIR spectra of both BAC and BAC-SiO_2 (Figure 2a) exhibited C-H stretching bands (2854 cm^{-1} and 2924 cm^{-1}) and C-H bending vibration band (1457 cm^{-1}), due to alkylammonium groups.[12–14] Asymmetric (1044 cm^{-1}) and symmetric (809 cm^{-1}) bands associated with Si-O-Si were observed in the spectra of BAC-SiO_2 before and after calcination.[20–21]

Quantification of BAC within the framework of BAC-SiO_2 was conducted using TGA (Figures 2b). Consistent with previous reports of quaternary ammonium surfactants, TGA data of freeze-dried BAC showed a 95 % weight loss in the range of 170-300 °C due to its thermal degradation (Figure 2b).[20, 22] On the other hand, the TGA curve of BAC-SiO_2 exhibited four distinct weight loss ranges: 1) the loss of water, and maybe residual ammonia from the synthesis, at < 170 °C; 2) first step of BAC degradation in the range of 170-300 °C; 3) second step of BAC degradation in the range of 300-340 °C; and 4) loss of water due to condensation of silanol groups. The weight loss between 170-340 °C was *ca.* 36% (0.56 g

per 1 g SiO_2), which corresponds to the amount of BAC within the BAC-SiO_2. The thermal properties of the materials were analyzed by DSC (see Figure S3).

TEM micrograph of the calcined material (Figure 2c) showed seemingly disordered mesopores structures with pore widths on the order of 30-50 Å. The small-angle X-ray diffraction (SAXRD) pattern (Figure 2d) was characteristic of an isotropic material that forms layers by virtue of consistent size rather than by extended 1D or 2D periodic arrangements of molecules. (The TEM image and SAXRD pattern of the corresponding BAC-SiO_2 material, before calcination, are shown in Figures S4–S6). Thus, there was no diffraction pattern from self-assembly of molecular species. There was only random packing of nearest neighbor pores that gave rise to a consistent, but isotropic, scattering vector near 32 Å, which is the approximate distance between rows of pores. If the pattern was cubic, then the pore-to-pore centroids are what were measured. However, information gathered from TEM micrographs and expected packing arrangements of random spheres appeared to favor an hcp motif, making the observed value to be $\sqrt{3}$ / 2 times the average core-to-core distance. Thus, the average core-to-core distance was about 37 Å. By incorporating the Scherrer equation, the domain spacing was determined to be *ca.* 11 nm, which is consistent with three repeats of the 37 Å spacing (*i.e.*, on average there are triplets of pores that scatter).[23–24]

The N_2 sorption results revealed a type IV isotherm, with a capillary condensation step and type H4 hysteresis loop (Figure S6), which is characteristic of mesoporous materials. The Brunauer-Emmett-Teller (BET) surface area, the Barrett-Joyner-Halenda (BJH) average pore width, and the pore volume were found to be 1579 m^2g^{-1}, 18.4 Å, and 0.56 $cm^3\ g^{-1}$, respectively (see details in SI).[25,26] However, the Kruk-Jaroniec-Sayari (KJS) corrections on the data with cylindrical pore assumptions[27] yielded a pore width closer to 30 Å. The hysteresis loop also suggested the presence of larger mesopores (−100-500 Å) due to inter-particle gaps.

A kinetic study of BAC release from BAC-SiO_2 into an aqueous solution in static conditions indicates that the release rate strongly depends on the solution's pH (Figures S7–S12). Controlled release of drugs in physiological conditions is of particular interest since the pH of many healthy human tissues is between 6.2-74, but decreases to a value of *ca.* 5 or lower in presence of inflammation, around tumor sites, or at specific areas of the body.[28]

In solutions with pH 7.4, only 2.5 % of the encapsulated BAC was released from BAC-SiO_2 within 2-3 days (Figure 3a). Upon decreasing pH to 4.0, a larger portion of BAC (8.0 %) was released within the same time frame. These findings agree with the drug release kinetics data for MSNs reported in literature.[9,29,30] The increase in BAC release in acidic solution can be largely attributed to the replacement of cationic benzalkonium with H^+ ions at the Si-O^- sites. Drug release profiles at pH values of 4.0, 5.0, 6.5, and 7.4 (Figure 3a) suggest that the amount of BAC released is pH dependent in a range of 4.0-7.4. It is important to note that although the majority (*ca.* 93 %) of the BAC remained within the particles, a second release profile (not shown) indicated an additional 4.5 % of BAC was released upon placing the particles in a fresh solution with pH 4.0. This and additional experiment (Figure S12)

suggested that the BAC could be continuously released from BAC-SiO_2 in physiologically-relevant dynamic conditions.

In order to investigate the mechanism of BAC release, the *in vitro* drug release data was analyzed using the power law (Korsmeyer-Peppas) model (Eqn. 1).[21,31] This model, based on Fick's second law of diffusion, depicts drug release with the assumption that the diffusion coefficient is concentration independent and the drug is homogeneously distributed throughout the drug delivery system. The general form is:

$$\frac{M_t}{M_\infty} = kt^n \quad \text{Eqn. 1}$$

where M_t and M_∞ are the cumulative amounts of released BAC at time t and infinity, respectively; n is the release exponent that characterizes the desorption mechanism; and k is the kinetic constant which correlates directly with the diffusion coefficient, D, if a constant thickness of the diffusion path is assumed.[32–33] Although the values of n are geometry dependent, the same BAC-SiO_2 material was used for the release experiments, eliminating the geometry variable. A plot of $\log(M_t/M_\infty)$ as a function of $\log(t)$, with $t \leq 62$ h in solutions with pH 4.0 and 7.4, (see Supporting Information or SI) yielded n values shown in Table S1.

Comparison of n values indicated that there were at least two processes that could govern the release of BAC from the silica particles. In phosphate-buffered saline (PBS) pH 7.4, n = 0.72, which is indicative of non-Fickian diffusion with a superposition of framework swelling or erosion.[21] However, in PBS solutions acidified with HCl to pH 4.0, 5.0, and 6.5, n values ranged between 0.13–0.18 which suggests non-Fickian diffusion from disordered pores with respect to shape, length, and size.[17,21] It is noteworthy that the dependence of n values to the release should, in reality, comprise several superimposed processes. For example, penetration of water into the particles is present in both release media, but it is more profound in PBS without HCl.

Kinetic modeling of the release data (see SI) demonstrated that the release mechanism in a solution with pH 7.4 versus that with pH 4.0 was different. The proposition of different mechanisms responsible for BAC release in the aforementioned media was reasonable due to the vast differences in the release environment. At pH 7.4, an environment representative of extracellular healthy tissues and blood, there is an excess of OH^- relative to H_3O^+ ions. Thus, the excess OH^- ions have the capacity to deprotonate some of the silanol (-Si-OH) groups and even hydrolyze some of the siloxanes. Many studies report that the pK_a of silanol groups is *ca.* 4-5.[34–35] On the other hand, at pH 4.0 the environment is moderately acidic, and thus, the electrostatically-bound BAC templates can be liberated by ion exchange with another cation (*e.g.*, H^+). Additionally, acid-catalyzed condensation of two silanol groups, which reduces silanol groups, occurs concomitantly with the release of the cationic BAC surfactants.

Since surfactant-extracted MSNs have proven to exhibit a remarkably faster degradation rate in simulated body fluid,[36] it is proposed that the materials synthesized herein will continue to release drug. Additionally, as the material is not calcined, the density of surface silanols is conserved, which can be further modified. Indeed, BAC-SiO_2 exposure resulted in a time- and concentration-dependent killing of the Gram-positive *S. aureus* and the Gram-negative *S. enterica* human bacterial pathogens (Figure 3b). Similar findings have been reported for BAC.[37,38] Importantly, SiO_2 had no effect on bacterial viability while BAC-SiO_2 displayed much more killing than pure BAC, when the amount of BAC present in and released from the BAC-SiO_2 was taken into consideration (40 wt.% BAC in BAC-SiO_2 that released <10% BAC in 2.5 days) (Figures 3a and 3c). Besides, any possible residual NH4OH in the material had no contribution to BAC-SiO_2's bactericidal activity (Figures S13 and S14 and discussions therein). These results, as a whole, suggest that BAC-SiO_2 is inherently quite effective at killing microbes.

In summary, we have developed a mesostructured silica drug delivery vehicle that releases BAC slowly over 2-3 days using pH changes as a trigger in static conditions. The material exhibits a high drug loading capacity and very good antibacterial properties. The synthetic approach can be extended to a variety of drugs to realize advanced functional biomaterials.

Supplementary Material

Refer to Web version on PubMed Central for supplementary material.

ACKNOWLEDGMENT

The authors thank Dr. Thomas J. Emge at Rutgers University and Dr. Xiaobing Zuo at Advanced Photon Source at Argonne National Laboratory for expert assistance in X-ray diffraction and scattering experiments, respectively. Additionally, the authors thank Prof. Michal Kruk at College of Staten Island, CUNY, for his invaluable advice on N_2 sorption data analysis. Hassan Al-Tameemi thanks the Government of Iraq for providing him with financial support to study at Rutgers University in USA.

REFERENCES

1. Wan Y; Zhao D Chem. Rev 2007, 107 (7), 2821–2860. [PubMed: 17580976]
2. Tang F; Li L; Chen D Adv. Mater 2012, 24 (12), 1504–1534. [PubMed: 22378538]
3. Joo SH; Park JY; Tsung C-K; Yamada Y; Yang P; Somorjai GA Nat. Mater 2009, 8 (2), 126–131. [PubMed: 19029893]
4. Feng X; Fryxell GE; Wang LQ; Kim AY; Liu J; Kemner KM Science 1997, 276 (5314), 923.
5. Yantasee W; Fryxell GE; Conner MM; Lin Y J. Nanosci. Nanotechnol 2005, 5 (9), 1537–40. [PubMed: 16193970]
6. Wen J; Yang K; Liu F; Li H; Xu Y; Sun S Chem. Soc. Rev 2017, 46 (19), 6024–6045. [PubMed: 28848978]
7. Zhaowei C; Chuanqi Z; Enguo J; Haiwei J; Jinsong R; P BB; Xiaogang Q Adv. Mater 2016, 28 (8), 1682–1688. [PubMed: 26684519]
8. Yu T; Enguo J; Jinsong R; Xiaogang Q Adv. Mater 2015, 27 (6), 1097–1104. [PubMed: 25655182]
9. Vallet-Regi M; Rámila A; del Real RP; Pérez-Pariente J Chem. Mater 2001, 13 (2), 308–311.
10. Lu J; Liong M; Li Z; Zink JI; Tamanoi F Small 2010, 6 (16), 1794–1805. [PubMed: 20623530]
11. Zhao Y; Trewyn BG; Slowing II; Lin VSY J. Am. Chem. Soc 2009, 131 (24), 8398–8400. [PubMed: 19476380]

12. Moulari B; Pertuit D; Pellequer Y; Lamprecht A Biomaterials 2008, 29 (34), 4554–4560. [PubMed: 18790531]
13. Wen J; Yang K; Xu Y; Li H; Liu F; Sun S Sci. Rep 2016, 6, 38931 (1-10). [PubMed: 27941942]
14. Wen J; Yan H; Xia P; Xu Y; Li H; Sun S Sci. China Chem 2017, 60 (6), 799–805.
15. Dement'eva OV; Frolova LV; Rudoy VM; Kuznetsov YI Colloid J. 2016, 78 (5), 596–601.
16. Dement'eva OV; Roumyantseva TB; Rudoy VM Colloid J. 2016, 78 (2), 281–284.
17. Dement'eva OV; Senchikhin IN; Kartseva ME; Ogarev VA; Zaitseva AV; Matushkina NN; Rudoy VM Colloid J. 2016, 78 (5), 586–595.
18. Nandni D; Mahajan RK J. Surfact. Deterg 2013, 16 (4), 587–599.
19. Russel AD; Hugo WB; Ayliffe GAJ, Principles and practice of disinfection, preservation, and sterilization. 3rd ed; Blackwell Science, University Press: Cambridge, United Kingdom, 1999.
20. Dement'eva OV; Rudoy VM RSC Adv. 2016, 6 (42), 36207–36210.
21. Fidalgo A; Lopez TM; Ilharco LM J. Sol-Gel Sci. Technol 2009, 49 (3), 320–328.
22. Dement'eva OV; Vinogradova MM; Frolova LV; Ogarev VA; Kuznetsov YI; Rudoy VM Colloid J 2014, 76 (1), 19–24.
23. Scherrer P, Nachr. Ges. Wiss. Gottingen 1918, 26, 98–100.
24. Langford JI; Wilson AJC J. Appl. Crystallogr 1978, 11 (2), 102–113.
25. Brunauer S; Emmett PH; Teller E J. Am. Chem. Soc 1938, 60 (2), 309–319.
26. Barrett EP; Joyner LG; Halenda PP J. Am. Chem. Soc 1951, 73 (1), 373–380.
27. Kruk M; Jaroniec M Chem. Mater 2001, 13 (10), 3169–3183.
28. Nazir S; Hussain T; Ayub A; Rashid U; MacRobert AJ Nanomedicine 2014, 10 (1), 19–34. [PubMed: 23871761]
29. Song SW; Hidajat K; Kawi S Langmuir 2005, 21 (21), 9568–9575. [PubMed: 16207037]
30. Ng JBS; Kamali-Zare P; Brismar H; Bergström L Langmuir 2008, 24 (19), 11096–11102. [PubMed: 18767822]
31. Qu F; Zhu G; Lin H; Sun J; Zhang D; Li S; Qiu S Eur. J. Inorg. Chem 2006, (19), 3943–3947.
32. Peppas N, Pharm. Acta. Helv 1985, 60, 110–111. [PubMed: 4011621]
33. Peppas NK RW, Hydrogels in medicine and pharmacy. CRC Press: Boca Raton, 1986; Vol. 3.
34. Leung K; Nielsen IMB; Criscenti LJ J. Am. Chem. Soc 2009, 131 (51), 18358–18365. [PubMed: 19947602]
35. Sulpizi M; Gaigeot M-P; Sprik M J. Chem. Theory Comput 2012, 8 (3), 1037–1047. [PubMed: 26593364]
36. He Q; Shi J; Zhu M; Chen Y; Chen F Microporous Mesoporous Mater. 2010, 131 (1), 314–320.
37. Morrissey I; Oggioni MR; Knight D; Curiao T; Coque T; Kalkanci A; Martinez JL PLOS ONE 2014, 9 (1), e86669. [PubMed: 24466194]
38. Furi L; Ciusa ML; Knight D; Di Lorenzo V; Tocci N; Cirasola D; Aragones L; Coelho JR; Freitas AT; Marchi E; Moce L; Visa P; Northwood JB; Viti C; Borghi E; Orefici G; the BIOHYPO Consortium; Morrissey I; Oggioni MR Antimicrob. Agents Chemother 2013, 57 (8) 3488–3497. [PubMed: 23669380]

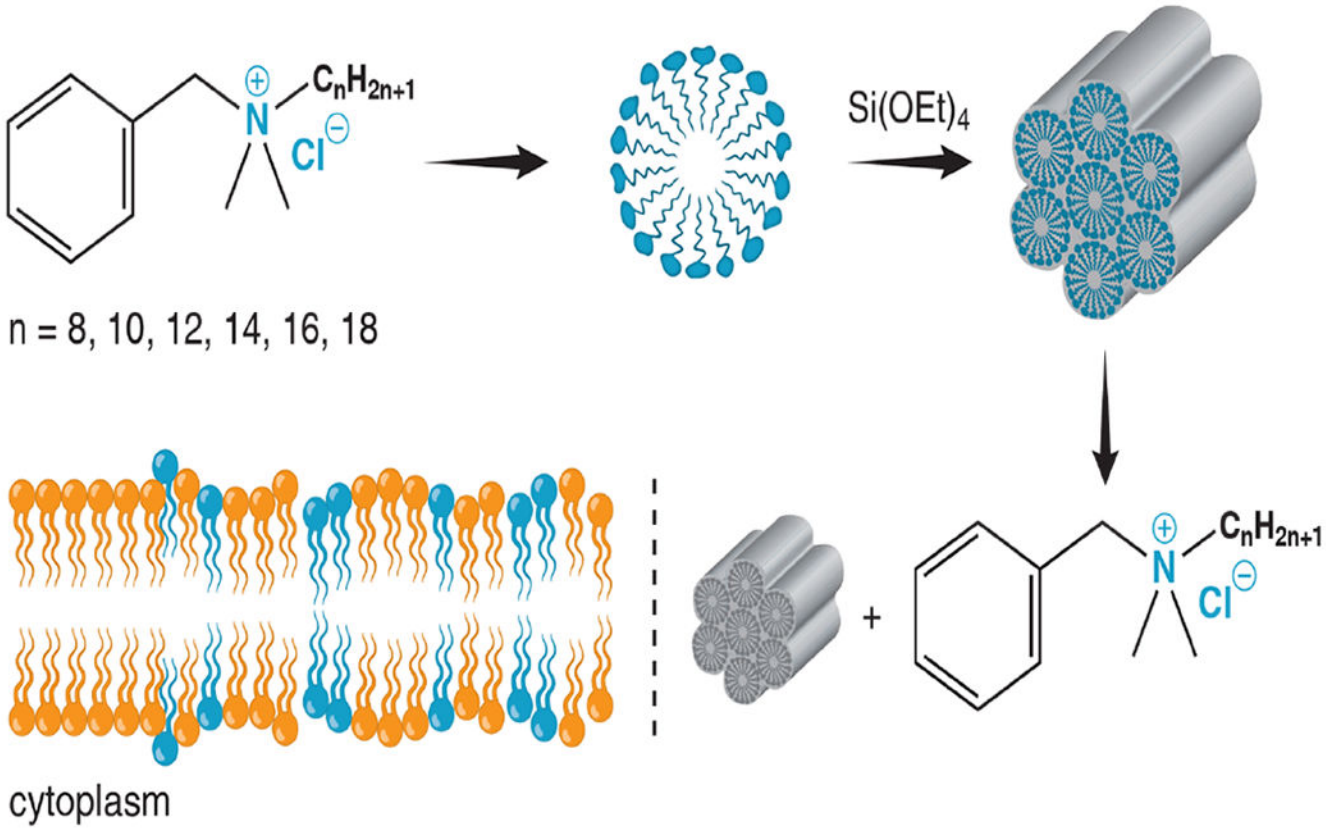

Figure 1.
Schematic illustration of the synthetic procedure, drug release, and antimicrobial mode of action of BAC-SiO_2.

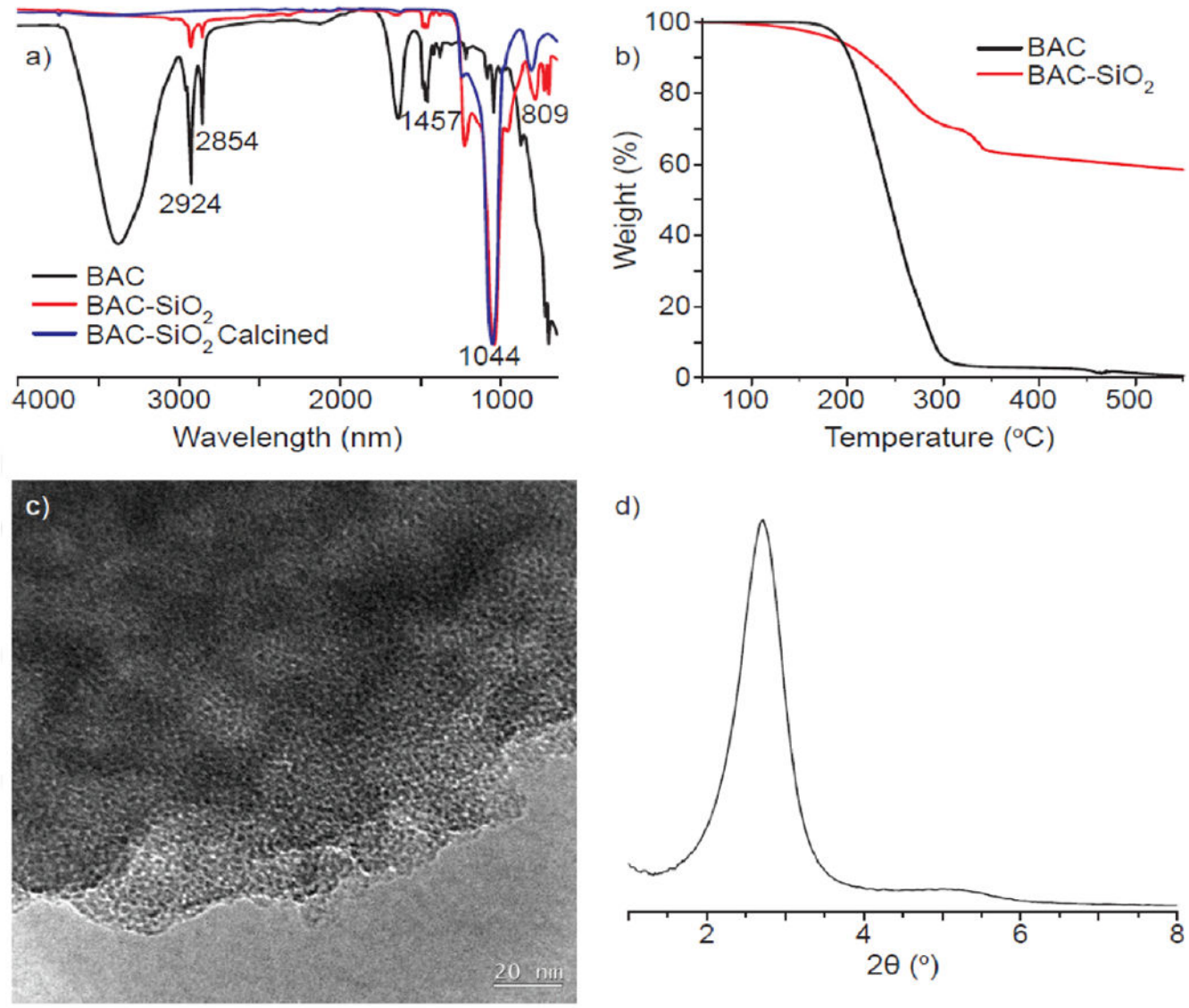

Figure 2.

a) ATR-FTIR spectra of lyophilized BAC, BAC-SiO_2, and calcined BAC-SiO_2; b) thermogravimetric analysis (TGA) curves of lyophilized BAC and as-synthesized BAC-SiO_2; c) HR-TEM micrograph of calcined BAC-SiO_2; and d) SAXRD pattern of calcined BAC-SiO_2.

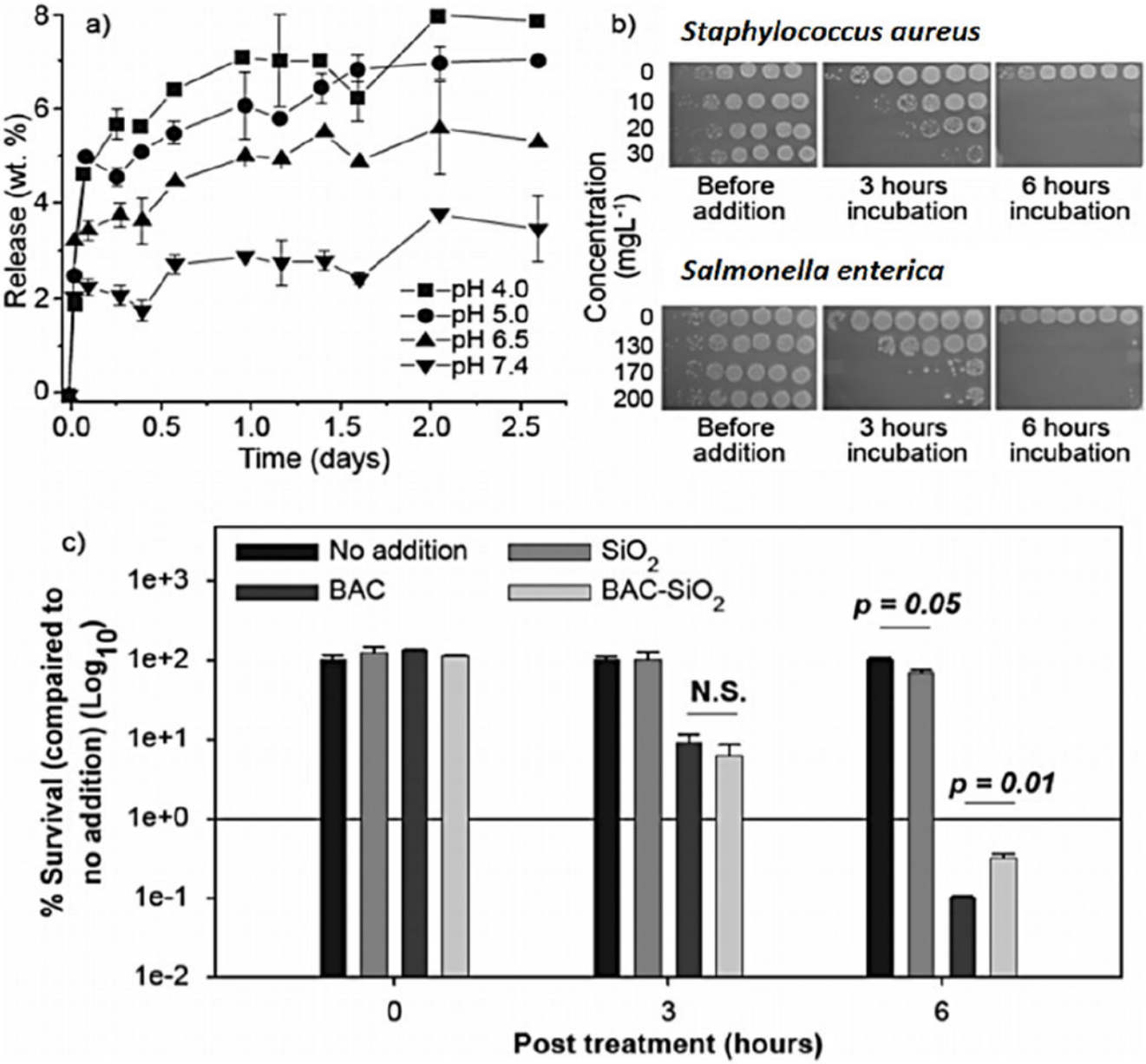

Figure 3.

a) Release profile of BAC from BAC-SiO_2 in PBS solution at pH 4.0, 5.0, 6.5, and 7.4 along with the corresponding standard deviation. b) Time- and dose-dependent killing of *S. aureus* and *S. enterica* by BAC-SiO_2. Photograph display of drop plates containing 10-fold serial dilutions (right to left: 10^0 to 10^{-6}) of treated cultures. c) The percentage of *S. aureus* survival upon exposure to 12 mg L^{-1} SiO_2, 4 mg L^{-1} BAC, or 10 mg L^{-1} BAC-SiO_2 for 0, 3, and 6 h is shown. Bacterial killing is monitored in triplicates. The average survival is displayed, in which error bars denote standard deviations. Statistical significance is calculated using a two-tailed t-test with significant p-values shown. “N.S.” denotes “not significant.”